Earth and Environmental Science Transactions of the Royal Society of Edinburgh, **106**, 185–197, 2016 (for 2015)

Clay mineralogical characteristics and the palaeoclimatic significance of a Holocene to Late Middle Pleistocene loess–palaeosol sequence from Chaoyang, China

Zhong-Xiu Sun[1], Qiu-Bing Wang[1*], Chun-Lan Han[1], Qing-Jie Zhang[1] and Phillip R. Owens[2]

[1] College of Land and Environment, Shenyang Agricultural University, Shenyang, Liaoning, 110866, P. R. China.
Email: sun19871001@126.com; wangqbsy@yahoo.com; hancly@163.com; zhangqingjie1010@163.com
[2] Department of Agronomy, Purdue University, West Lafayette, IN 47907, USA.
Email: sun19871001@126.com; prowens@purdue.edu
*Corresponding author.

ABSTRACT: Changes in soil chemistry in response to varying climatic regimes can alter the equilibria of soil systems and result in different clay minerals. Variations in phyllosilicate clay composition can reflect temporal and spatial climatic changes, such as summer/winter monsoon cycles. The objective of this research was to investigate the mineralogy of the clay fractions as a proxy for determining variations in the East Asian monsoon climate, based on a section at Chaoyang in China spanning the last 0.423 Ma BP. The clay mineralogy record in the Chaoyang section was compared with other proxies as recorded in this section and with other palaeoclimatic indicators, including oxygen isotopes from oceanic sediments and loess–palaeosol sections on the Chinese Loess Plateau (CLP). The results from clay mineralogy and related climatic studies show that the summer monsoon has a trend of four increased stages and four decreased stages; whereas the winter monsoon displays the opposite trend. During the last 0.423 Ma BP, the strongest winter monsoon occurred around 0.243–0.311 Ma BP. During this period, which included an intense winter monsoon, the soil in the section had the least illite, one of the smallest kaolinite and illite/Chlorite (I/C) indices and an overall decreasing clay content. The period 0.225–0.243 Ma BP had the strongest summer monsoon over the last 0.423 Ma BP. This period had the greatest amount of illite, the highest I/C index, greater overall clay content and the strongest magnetic susceptibility signal. Additionally, this section contained the smallest mean grain size. The multi-monsoon climate cycles of alternating cold-dry and warm-moist conditions as recorded in the Chaoyang section corresponded well with multiple glaciation cycles based on deep sea sediments. This indicates that the Chaoyang section provides a record of palaeoclimate changes in northeast China that can be linked to mineralogical suites to assist in reconstructing the palaeoclimate over the Late Middle Pleistocene, and complements the global palaeoclimate records in the CLP.

KEY WORDS: Chaoyang section; palaeoclimate reconstruction; palaeomonsoon; weathering

Public perceptions of climatic change and variability have been greatly influenced by regional climatic trends and extreme events. Climate change has become one of the most serious challenges posed to the world in the 21st Century (Bekryaev *et al.* 2010; Ackerley *et al.* 2011; Williams & Funk 2011; Wild 2012). In order to contribute to the understanding of this problem, it is necessary to consider climate simulations and predictions (Dole 2012). Understanding past climates is difficult because records of climate change are limited and there are not enough data to establish a comprehensive and reliable system for climatic simulation. Palaeoclimatic data are mainly derived from natural sources, including lake sediments, stalagmites, corals, tree rings, oceans, glaciers and dated loess–palaeosol sequences (Mintzer 1992; Jansen *et al.* 2007), which are mainly related to past climates in the Holocene (An *et al.* 1991a, b; Sun *et al.* 2006). Research on palaeoclimatic variations in the middle and late Pleistocene are less abundant and, overall, are less understood. Many processes affecting climatic change predate the Holocene. Thus, long-term data are needed to assist with the interpretation and prediction of climatic change over longer timescales.

Quaternary loess–palaeosols have an extensive global distribution (Pye 1984), record long-term climatic changes (Fink & Kukla 1977) and have been widely applied to studies of palaeoclimate (Heller & Liu 1982; Liu 1985; Liu & Ding 1998). Some researchers have made remarkable achievements in their studies of palaeoclimate, using loess–palaeosols from central China (Liu & Ding 1998), central United States (Hall & Anderson 2000) and central Europe (Fink & Kukla 1977). However, Quaternary climatic changes are varied and complex (Ding *et al.* 1999). Therefore, much more data are needed from different sites to enable the simulation and prediction of global climatic changes (Dole 2012).

The East Asian monsoon is an integral part of the global climatic system (An 2000) and its evolution is a principal and direct factor which controls palaeoenvironmental changes in East Asia (Liu 1985; Yang & Xu 1985; An 2000). The East Asian monsoon has two seasonally alternating monsoon

 doi:10.1017/S1755691016000098

circulations – the East Asian summer monsoon (EAS) and the East Asian winter monsoon (EAW) (Zhang & Lin 1987). China is located in East Asia and has been controlled by the East Asian monsoon climate over the last 2600 ka BP (Liu & Ding 1998; An 2000). Research on loess–palaeosols from central China has shown that palaeosols are associated with a southerly moisture-bearing EAS (An *et al.* 1991b), and loess is deposited dust which is transported by the northerly EAW under cold and dry conditions (Liu 1985; An *et al.* 1991a). These results help towards a better understanding of the evolution of the East Asian monsoon (An 2000). In 2006, an exposed loess–palaeosol section was discovered during investigations in the northwest of Liaoning province in China, about 1000 km from the Chinese Loess Plateau (CLP). The 19.85-m section was formed since 0.423 Ma BP, and contains many different loess and palaeosol layers. It was previously called the Fenghuangshan section (Chen *et al.* 2009a, b) and has been renamed the Chaoyang section to reflect recent research on the CLP (Kalm *et al.* 1996; Gylesjö & Arnold 2006). Grain size can be used as a proxy indicator of the sedimentary environment (Sun *et al.* 2000; Ding *et al.* 2001). Chen *et al.* (2009b) have conducted a systematic and intensive study of grain size characteristics of the Chaoyang section, using high resolution sampling (2 cm intervals). The dust source area is very sensitive to changes in continental aridity related to variations in global or regional atmospheric circulation (Vandenberghe *et al.* 1997; Kukla & An 1989). Dust deposits in thick loess can provide some of the most complete and detailed information on the effects of climatic change (Liu 1985; Pye 1987). The Chaoyang loess–palaeosol sequence was determined to be of aeolian dust origin and is very suitable for palaeoclimatic research (Chen *et al.* 2009b). This section originates from aeolian dust deposits and, thus, ought to record palaeoclimatic changes which occurred during the Quaternary. Because grain size should not be used on its own, more firm evidence from other proxies is also needed to reveal palaeoclimatic variations in the Chaoyang section over the Late Middle Pleistocene.

Previous studies have demonstrated that clay minerals can serve as sensitive and reliable proxies of climatic change, and can aid in understanding the evolution of the monsoon climate (Zhang & Yuan 1987; Peng 1988; Wang 1988; Kalm *et al.* 1996; Huang *et al.* 2011, 2012). Given that loess is a consistent parent material, any differences should indicate variations in weathering (Liu & Ding 1998), as reflected in the successive stages of mineralogical evolution (Turpault *et al.* 2008). Clay minerals can be taken to be a reliable proxy of palaeoclimates, because the morphology and substructure of clay minerals are very sensitive to environmental changes and have been demonstrated to record these changes in crystal structures (Wilson 1999; Chadwick *et al.* 2003; Velde & Meunier 2008; Velde 2012).

This study of the Chaoyang section is based on high-resolution sampling to investigate clay mineralogy, in order to identify variations in the monsoon climate and to evaluate the suitability of the Chaoyang section for palaeoclimatic research. The overall aim was to investigate the paleoclimate during the Late Middle Pleistocene and to propose a palaeoclimatic sequence for the CLP. Comparisons are made with climate changes as recorded in other proxies at the Chaoyang section, along with other palaeoclimatic records such as oxygen isotopes from oceanic sediments and from loess–palaeosol sections on the Chinese Loess Plateau (CLP).

1. Materials and methods

The Chaoyang section is situated at Chaoyang (N 41°33′9.6″, E 120°30′ 20.8″; Fig. 1), and is located in the northeast area of China's loess area. The modern mean annual temperature and mean annual precipitation are 9°C and 450–500 mm, respectively. The Chaoyang section is about 1334 km northeast of the Lingtai section (N 35°00′75″, E 107°30′33″; 9.1°C, 600 mm) (Gylesjö & Arnold 2006), about 1414 km northeast from the section at Baoji (N 34°24′, E 107°18′; 13°C, 700 mm) (Kalm *et al.* 1996), about 1349 km northeast from the Wugong section (N 34°19′17″, E 108°07′07″; 12–14°C, 650–750 mm) (Huang *et al.* 2012), and about 1542 km northeast of the Longxi section (N 34°56′, E 104°41′; 5.5–7.5°C, 400–600 mm). There is a climatic gradient from north to south with Chaoyang (9°C, 450–500 mm), Lingtai (9.1°C, 600 mm) and Baoji (13°C, 700 mm). The sections at Lingtai, Baoji, Wugong and Longxi are loess deposits on the Chinese Loess Plateau, and have been widely investigated as a continuous terrestrial palaeoclimate archive. The base rocks at Chaoyang are of Archean and Presinian age (Liaoning Geology Bureau, Hydrogeology Brigade 1983) and these underlie Paleozoic sedimentary rocks. The Paleozoic sedimentary rocks are mainly limestone and dolomite of Cambrian and Ordovician age (Liaoning Geology Bureau, Hydrogeology Brigade 1983). The Chaoyang section above these older formations originated as aeolian deposits (Chen *et al.* 2009b), with no pedogenic relationship with the underlying basal layer (Hu *et al.* 2010).

The studied profile was in a closed basin of the Fenghuangshan area that occurs at a midpoint on the Song Ling Ridge in the hilly area of western Liaoning. It was close to the drainage divide and was not subject to water erosion (Fig. 1). The catchment area is also small, and does not display evidence of human impact or accelerated erosion (Liaoning Geology Bureau, Hydrogeology Brigade 1983). As a result, the section and the palaeosols are well preserved.

Field stratigraphic correlation was by Chen *et al.* (2009b), based on widely applied stratigraphic markers for Chinese loess (Liu 1985; Kukla 1987). The Chaoyang section consists of a 19.85 m-thick loess deposit, comprising five soil couplets with 42 genetic horizons, with no observed bottom boundary. Layer S0 is a modern soil formed during the Holocene. The loess–palaeosol sequence was numbered from top to bottom as L1, S1, L2, S2, L3, S3, L4, S4 and L5 (Fig. 2a), where L represents loess and S stands for palaeosol. Stratigraphic descriptions were provided by Chen *et al.* (2009b) and 42 genetic horizons were described in detail by Sun *et al.* (2016). In order to characterise the stratigraphy of the loess–palaeosol sequence, a Bartington susceptibility meter (MS2), equipped with a MS2F probe, was used to directly measure mass magnetic susceptibility of the whole section in the field, with a precision of 1–2 %. The face of the profile was cleaned to create a fresh and smooth surface. Then we gently used a probe to vertically contact the measured surface every 2 cm in triplicate, in order to calculate the average value of magnetic susceptibility for each depth. The magnetic susceptibility data illustrate boundaries that generally correlate with the lithologic changes as differentiated in the field. The palaeosols within the Chaoyang section can easily be recognised by peaks in the magnetic susceptibility curve and laboratory data, which show increases in the <2 μm grain size (Fig. 2b). During field examination, the S0 and L1 were considered to have been reworked by water. Therefore, the top 2 m should be interpreted with care (Chen *et al.* 2009b; Sun *et al.* 2016).

The chronology of the Chaoyang section was dated by optically stimulated luminescence (OSL) and electron spin resonance dating (ESRD). Ten samples for dating were collected from the layer boundaries which were considered to be of significance. Samples were taken after dusk in order to avoid sunlight contamination. We removed a whole block of soil (about 500–1000 g) and immediately sealed it with

https://doi.org/10.1017/S1755691016000098 Published online by Cambridge University Press

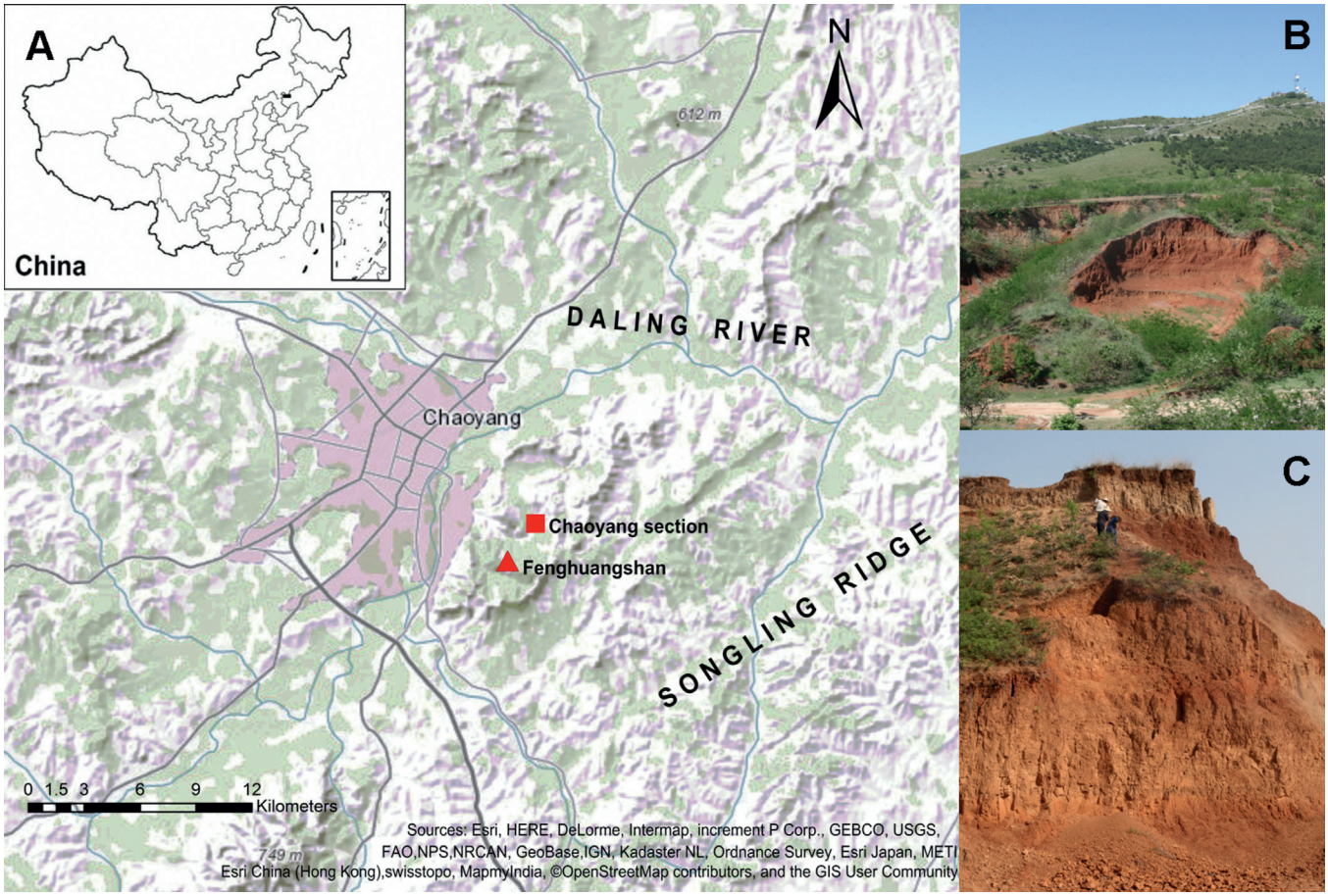

Figure 1 (A) Schematic map showing the location of the Chaoyang loess–palaeosol section. The black square on the inset map shows the location of Chaoyang in China. The schematic map was plotted using Arc GIS 10.2.2. (B) An image of the Chaoyang section and its associated landscape. (C) An image of the Chaoyang section.

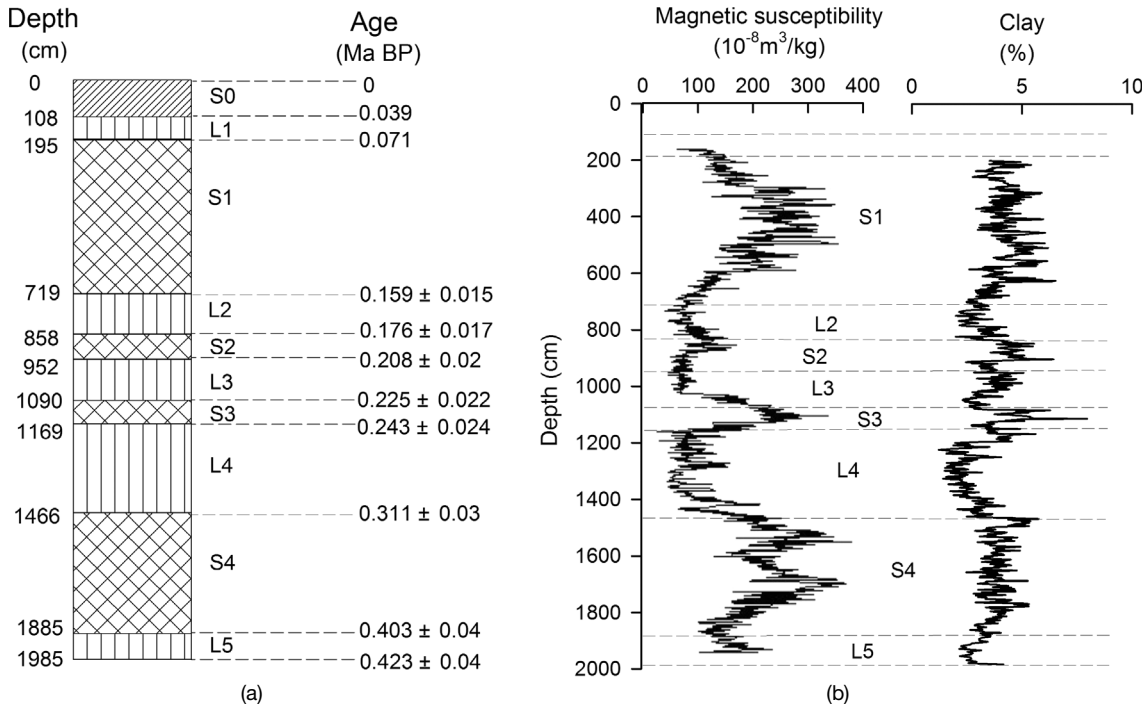

Figure 2 (a) Schematic logs of the stratigraphy with corresponding time constraints of the Chaoyang section. (b) The magnetic susceptibility and <2 μm grain size contents of the Chaoyang loess–palaeosol sequence.

https://doi.org/10.1017/S1755691016000098 Published online by Cambridge University Press

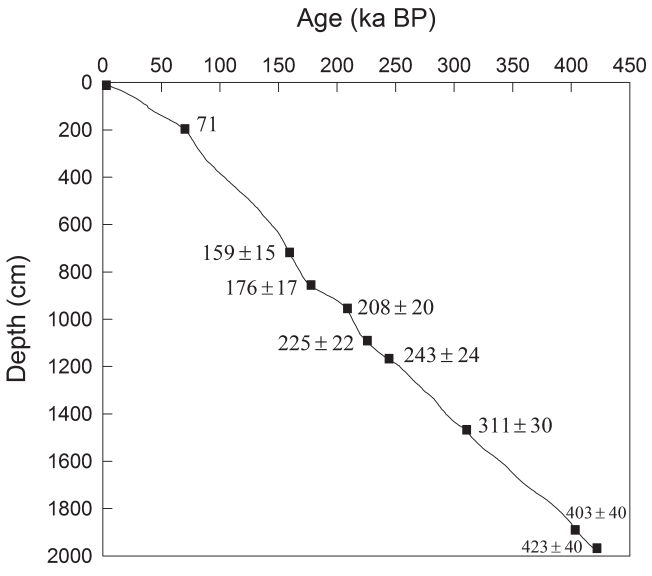

Figure 3 A diagram showing the age–depth relationship for the Chaoyang section, based on the age model of Kukla & An (1989).

aluminium foil, labelled the sample and placed it in a thick black plastic bag. The analysis was carried out in the State Seismological Bureau of China. There were no time reversal problems detected in the ten dating samples. After analysis, a chronology for the Chaoyang section was determined using ten reliable age controls, as interpolated from a susceptibility age model using the accumulation rate (Kukla & An 1989); the age–depth relationship for the Chaoyang section based on the age model of Kukla & An (1989) is depicted in Figure 3. The dating results for the Chaoyang section correlate well with the loess sequence on the Chinese Loess Plateau (Chen 2009). For example, the Lingtai section includes a loess formed during 0.039–0.071 Ma BP, which is consistent with the loess of L1 in the Chaoyang section.

Rare earth element (REE) concentrations of loess were measured using a Vista-MPX inductively coupled plasma atomic emission spectroscopy (ICP-AES) at Shenyang Agricultural University. A 100-mg sample powder was dissolved in a Teflon crucible, using $HCl–HNO_3–HF–HClO_4$. The standard reserve liquid from the China National Analysis Center for Iron and Steel was used to calibrate elemental concentrations in the samples. Analytical uncertainties involved in measurements are less than ± 5 % for REEs.

Twenty-two loess and 20 palaeosol samples from different genetic horizons were collected for mineralogical analysis, which should correlate well with the time series. First, <2 μm clay fractions were separated from the bulk sample. Organic matter was oxidised in 5 % H_2O_2 solution and calcium carbonate was removed by 1 M sodium acetate (pH5). The clay fractions were then collected by repeated settling in deionised water. Secondly, free Al- and Fe-oxides from clay fractions were removed by dithionite–citrate–bicarbonate treatment (Mehra & Jackson 1958) and centrifuging. Then, for mineralogical analysis, clay samples were (1) air-dried; (2) saturated with 0.5 M Mg^{2+}; (3) saturated with 1 M K^+; and (4) treated with 2 M HCl. After the clay treatments, oriented mounts were prepared as slurries on glass slides by smearing a clay paste onto a glass slide (Theisen & Harward 1962; Gibbs 1965). The Mg solutions were evaluated in the air-dried state and then glycerol saturated at 25°C for 24 h (Mg-glycerol). The K-saturated samples were run in the air-dried state at 25°C for 24 h (K-25°C), heated to 300°C for 2 h (K-300°C), and then heated to 550°C for 2 h (K-550°C). The specimens were treated with 2 M HCl in an air-dried state at 80°C for 2 h. Rehydration was avoided by cooling the specimen in a desiccator. Finally, samples from different treatments, including Mg-glycerol, K-25°C, K-300°C, K-550°C and HCl-80°C, were examined respectively by a Bruker D8 X-ray Diffractometer, using CuKα radiation generated with 40 kV, 40 mA tube currents, and scanned from 2° (2θ) to 30° (2θ) at a scanning speed of 2° (2θ) min^{-1}. The individual phyllosilicate minerals were identified by their basal reflection characteristics as listed in Table 1.

For semi-quantitative analysis, the integrated characteristic peak areas of individual mineral reflections (Pai *et al.* 1999) were converted into percentage relative abundances by using empirically estimated weighting factors (Brindley 1980). The relative quantities aid comparisons with other results.

2. Results

2.1. Clay mineralogy of the Chaoyang section

The clay mineral compositions of the Chaoyang section as a function of depth are plotted and listed in Figure 4. In general, illite (40–70 %) dominates the clay fraction, as compared to vermiculite (20–40 %), kaolinite (6–15 %) and chlorite (2–15 %), and minor amounts of smectite (0–10 %) occur throughout the entire section. The average weight percentages of clay minerals in the entire section are illite (45 %), vermiculite (38 %), chlorite (4 %), kaolinite (11 %) and smectite (2 %).

2.2. Trends in illite content

On average, the illite concentration (48 %) in the Chaoyang section is similar to that in the Lingtai section (49 %) and lower than the 66 % for the Baoji section in S1–L5. The illite contents in loess (L1–L5) and palaeosols (S0–S4) are 39 % and 53 %, respectively, which is similar to the abundance of illite in the Lingtai section (46 %, 51 %) (Gylesjö & Arnold 2006), and also to the Longxi section (50–70 %) (Zheng 1982). However, the Chaoyang section has lesser amounts of illite when compared to the Baoji section (71 % loess, 63 % palaeosol) (Kalm *et al.* 1996). On average, the illite concentrations of all layers in L2–L5, S1–S4 and L1 are around 47 %. The average illite contents in loess layers in L2–L5 and palaeosol layers in S1–S4 in the Chaoyang section are about 38 % and 61 %, respectively. The average illite content of L2–L5 loess in the Chaoyang section is similar to that in the Lingtai section, but significantly less than in the Baoji section (72 %). The S1–S4

Table 1 X–ray diffraction characteristics of several major clay minerals (nm)

Minerals	Air-dried	Mg-glycerol	K-25 °C	K-300 °C	K-550 °C	HCl-80 °C
Smectite	1.5–1.55	1.8	1.0–1.2	1.0–1.2	0.96–1.0	1.2–1.5
Vermiculite	1.42	1.42	1.0	1.0	0.93	1.42
Illite	1/0.5/0.33	1.0/0.5/0.33	1.0/0.5/0.33	1.0/0.5/0.33	1.0/0.5/0.33	1.0/0.5/0.33
Kaolinite	0.715–0.72/0.358	0.715–0.72/0.358	0.715–0.72/0.358	0.715–0.72/0.358	0	0.715–0.72/0.358
Chlorite	0.71/0.47/0.353	0.71/0.47/0.353	0.71/0.47/0.353	0.71/0.47/0.353	0.71/0.47/0.353	0

Notes, data were cited from Brown & Brindley (1980), Srodon & Eberl (1984), Thorez (1976), Moore & Reynolds (1989), and Li (1997).

https://doi.org/10.1017/S1755691016000098 Published online by Cambridge University Press

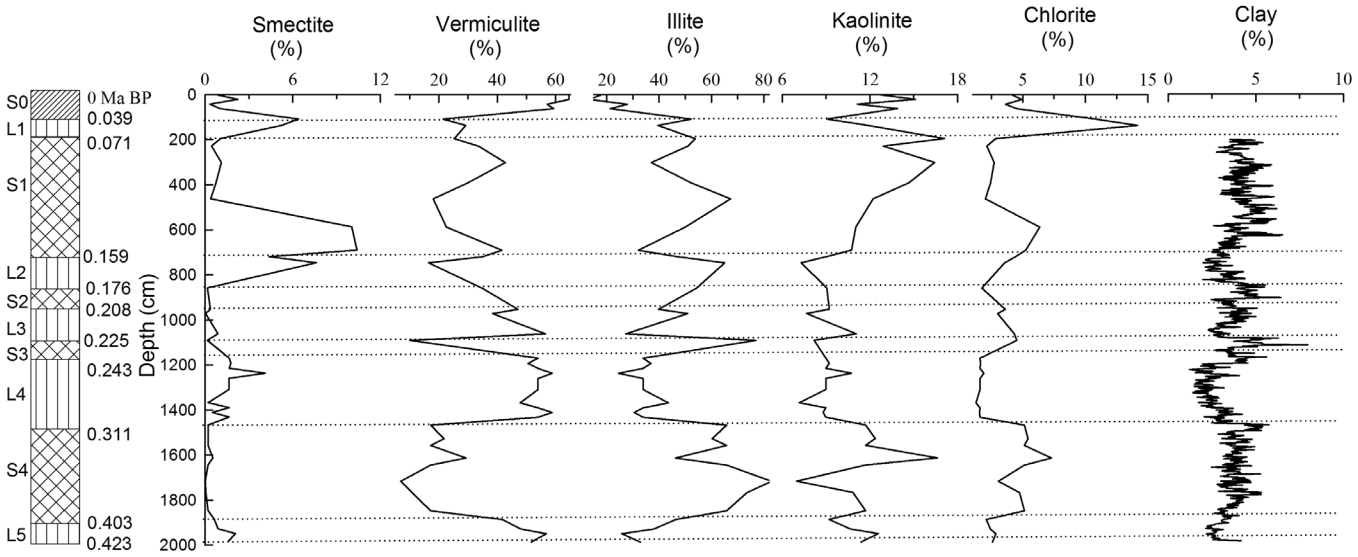

Figure 4 Mineralogy in weight percent of the clay fraction and the weight percent of <2 μm grain size fraction from the loess–palaeosol sequence of the Chaoyang section.

palaeosol is similar to the Baoji section (63 %), but significantly greater than the Lingtai section (51 %).

Illite concentrations exhibit an increase throughout L5 to L2 and a decrease in palaeosols from S3 to S1 (Fig. 4). The S0 (20 %) has the lowest illite concentration when compared to the whole Chaoyang section. Lower illite concentrations were found for loess compared to palaeosols (except S0) in Chaoyang, and this difference is consistent with the Lingtai loess section during 0.039 to 0.423 Ma BP (Fig. 4). Variations in clay minerals can generally be noted around the transition between different units. As with the Lingtai section, there is a stepwise decrease in illite across the S1–L1 boundary (52–46 %), whereas the chlorite content increases. Also, in L1 the chlorite abundance exhibits the greatest average value. The S3 has the lowest average kaolinite concentration (8 %) within the whole Chaoyang section (Fig. 4). There is an increase in illite from L4 to S3 and there is a maximum of up to 77 % at S3. The same trends were observed in both the Lingtai and Baoji sections, where S3 has an illite content of around 50 %. These data indicate that S3 should be a key location for investigating the relationship between clay mineralogy and climate as reflected in temperature and precipitation. A significant increase in illite is shown in S0 across the Chaoyang (20 %), Lingtai (48 %) and Baoji (65 %) sections along the climate gradient, in accordance with the average illite concentrations in S1–L5.

2.3. Trends in chlorite

A significant decrease in chlorite is shown in S1–L5 and S0 in the Chaoyang (3.2 %, 4.3 %), Lingtai (2.3 %, 2.6 %) and Baoji ($\leq$2 %, <1 %) sections. The average chlorite abundance in palaeosols of the Chaoyang section is about 4 %, which is only slightly greater than for loess (3.6 %). L1 has the greatest percentage of chlorite among the units; contrarily, S1–L5 contain the lowest on average, which is similar to the Lingtai and Baoji sections. Vermiculite concentrations in L1 exhibit an abrupt decrease from the initial layer S0 at about 40 %, whereas the chlorite content increases to approximately 30 % during the last 0.071 Ma BP. Similarly, Huang *et al.* (2012) found the same regular pattern in the Wugong section. However, there is a decrease to the lowest chlorite content in L4. There is a general trend, with an increase that is evident upwards in the section to the L2 loess.

2.4. Trends in smectite

Smectite was found in small amounts and with little change, varying from trace to less than 10 % throughout the section, and displaying a decrease to nearly zero in the palaeosol when compared to loess. For the Lingtai section, the value is similar to the Chaoyang section and is around 3 % for loess. An abrupt decrease was found from L2 to S1 in the Chaoyang section, and this pattern was also observed in both the Lingtai and Wugong sections.

2.5. Trends in kaolinite

The entire section shows little change in the relative proportions of kaolinite which ranges from 9 % to 15 % (Fig. 4) and is not more than 15 % for the Baoji (Kalm *et al.* 1996), Heimugou (Zheng 1982) and Lingtai sections (Gylesjö & Arnold 2006). The average quantities are slightly greater in palaeosols (12 %) than in loess (10 %). S1–L5 is characterised by approximately 3 % less kaolinite in loess than in palaeosols (Fig. 4). This trend coincides with the Baoji section. It is notable that the amounts of kaolinite in L1 and L2–L5 increase progressively in the Chaoyang, Lingtai and Baoji sections along the climate gradient, which parallels decreasing chlorite.

Figure 4 displays a greater amplitude in mineral phase variability; this can be generally observed within palaeosols compared to loess, with the largest and smallest amounts in S3 and L4 respectively. The characteristics of the detailed mineralogical distribution in the Chaoyang section in terms of illite and clay fraction show broadly the same trend, with different amplitudes in palaeosols and decreases in loess. Chlorite concentrations demonstrate a trend which is opposite to the illite trend (Fig. 4).

3. Discussion

3.1. Clay weathering

Four other lines of evidence support comparison of clay mineral trends. First, throughout the Chaoyang section, the rare earth element (REE) distribution patterns are very similar, including negative slopes where the main enrichment was found in Ce (Fig. 5). In Figure 5, the Eu–Lu curve is relatively smooth and the La–Eu curve is steep. The similar trends between the loess and palaeosols indicate they have similar provenance during the last 0.423 Ma BP. Analogous patterns can be observed

https://doi.org/10.1017/S1755691016000098 Published online by Cambridge University Press

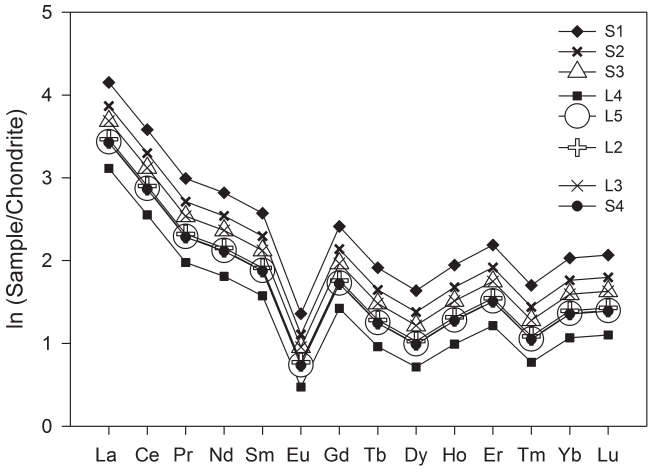

Figure 5 Chondrite-normalised rare earth element patterns of the Chaoyang section. Data are cited from Chen *et al.* (2009a). Abbreviations along the X axis: La = Lanthanum; Ce = Cerium; Pr = Praseodymium; Nd = Neodymium; Sm = Samarium; Eu = Europium; Gd = Gadolinium; Tb = Terbium; Dy = Dysprosium; Ho = Holmium; Er = Erbium; Tm = Thulium; Yb = Ytterbium; Lu = Lutetium. The symbols for different loess–palaeosol sections can be found in the Methods section and Figure 2.

with the REE distribution of the Linghui section (Feng *et al.* 2011) from the CLP. Although the source region is poorly known in detail, the Chaoyang section should be comparable with sections on the CLP. There should be no distinct alteration before loess deposition (Jeong *et al.* 2008). The S1 to L5 part of the Chaoyang section has typical properties for loess with a uniform parent material, in terms of field morphology, particle size distribution, geochemistry and micromorphology (Sun *et al.* 2016). Post deposition, the clay mineralogy changes were derived from weathering (Schaetzl & Anderson 2005). Therefore, for this study it is assumed that the processes of pedogenesis are more important than the loess source. Secondly, the constituents of phyllosilicate minerals in the Chaoyang, Lingtai (Gylesjö & Arnold 2006) and Baoji (Kalm *et al.* 1996) sections are dominated by illite, with different abundances of chlorite, kaolinite and smectite throughout the profiles. These results accord with results from other loess–palaeosol research on the CLP, such as that on the Wugong section (Huang *et al.* 2012). Thirdly, the loess source was completely mixed before final deposition, to form the rather uniform mineralogy (Jeong *et al.* 2011) with very little weathering occurring during transportation (Jeong *et al.* 2008). Fourthly, there are identical trends in magnetic susceptibility in the Chaoyang, Lingtai and Baoji sections. Thus, we can conclude that clay minerals from these sections are comparable.

In East Asia, the palaeoenvironmental changes were primarily controlled by the evolution of the East Asian monsoon (An 2000). As a particular climate and soil environment are necessary for the formation or preservation of certain clay minerals (Folkoff & Meentemeyer 1987; Amundson *et al.* 1989; Velde 2012), the major differences between the loess–palaeosol sequences are related to the mineralogical changes in phyllosilicate composition (Jeong *et al.* 2011) and are sensitive to environmental change to affect pedogenesis. Clay mineralogy is very much influenced by parent material under a specific bioclimate (Folkoff & Meentemeyer 1985, 1987). With increasing time, the ions in the parent material determine the potential for specific clay mineral formation. In this slow process, chemical weathering affects the soil mineralogy, subject to any constraints imposed by the climate. Environmental conditions can determine which clay mineral suites may develop. Therefore, clay mineralogy usually reflects climatic conditions (Arkley 1963, 1967; Van der Merwe & Weber 1963; Grim 1968; Folkoff & Meentemeyer 1987; Velde 2012), but can also be modified by the biota (Schaetzl & Anderson 2005). In a classic study on soil data for 99 US representative pedons by the National Soils Testing Laboratory in Lincoln, Nebraska, Fiskell & Perkins (1970) and Folkoff & Meentemeyer (1987) used regression equations to demonstrate the strong link between clay mineralogy and climate. The primary link between clay minerals and environment is dependent on the leaching and weathering regimes (Beaven & Dumbleton 1966; Rai & Lindsay 1975). Increased leaching tends to decrease silica activity and increase weathering. In this region of China, leaching and weathering are primarily driven by monsoon-associated precipitation under a continental monsoonal climate. Temperature mainly affects the rate of the weathering, not the direction within a mineralogical suite (Rai & Lindsay 1975; Li *et al.* 2008). Precipitation and temperature are the main controls on seasonal leaching and drying in soils, also affected by clay mineralogy (Folkoff & Meentemeyer 1985; Chadwick *et al.* 1995). In China, the magnitude of seasonal leaching and drying are closely associated with the East Asian monsoon climate, with distinct seasonal changes in precipitation and air temperature between cold-dry (winter monsoon) and hot-humid (summer monsoon) (Ding & Yu 1995; An 2000). Thus, variations in phyllosilicate composition in loess–palaeosol sequences can be used to infer temporal and spatial changes in mineral evolution and the strength of the summer/winter monsoon.

3.2. The evolution of clay minerals

As has been demonstrated by other researchers (Table 2), smectite prevails in areas with poor drainage in temperate soils (Dixon & Weed 1989); whereas illite commonly dominates in cold climate soils (White & Blum 1995; Velde & Meunier 2008). Chlorite can be relatively unstable and easily changed under intense precipitation (Chadwick *et al.* 2003; Velde & Meunier 2008). Kaolinite can form under intense weathering in warm and moist environments, and is common in areas with subtropical or tropical climates (Dixon & Weed 1989; White & Blum 1995). Vermiculite is a fast-forming and unstable intermediate mineral which is derived initially from mica and can be transformed to form smectite or other minerals, depending on the environment (Wilson 1999; Velde & Meunier 2008). Therefore, palaeosols formed under a warm and humid climate should contain smaller amounts of chlorite and greater amounts of illite and kaolinite.

Illite is generally the most common mineral in the Chaoyang section, as well as at Lingtai and Baoji, which indicates that

Table 2 General relationships between clay types and climatic conditions

Climatic-signal/type	Clay mineral types	Weathering sequence	Citations
Cold climate	Illite	↓	Dixon & Weed (1989); Velde & Meunier (2008)
Temperate climate with poor drainage	Smectite		White & Blum (1995); Chadwick *et al.* (2003)
Subtropical or tropical climate	Kaolinite		Wilson (1999)
Tropical climate	Fe oxides and Al oxides		

https://doi.org/10.1017/S1755691016000098 Published online by Cambridge University Press

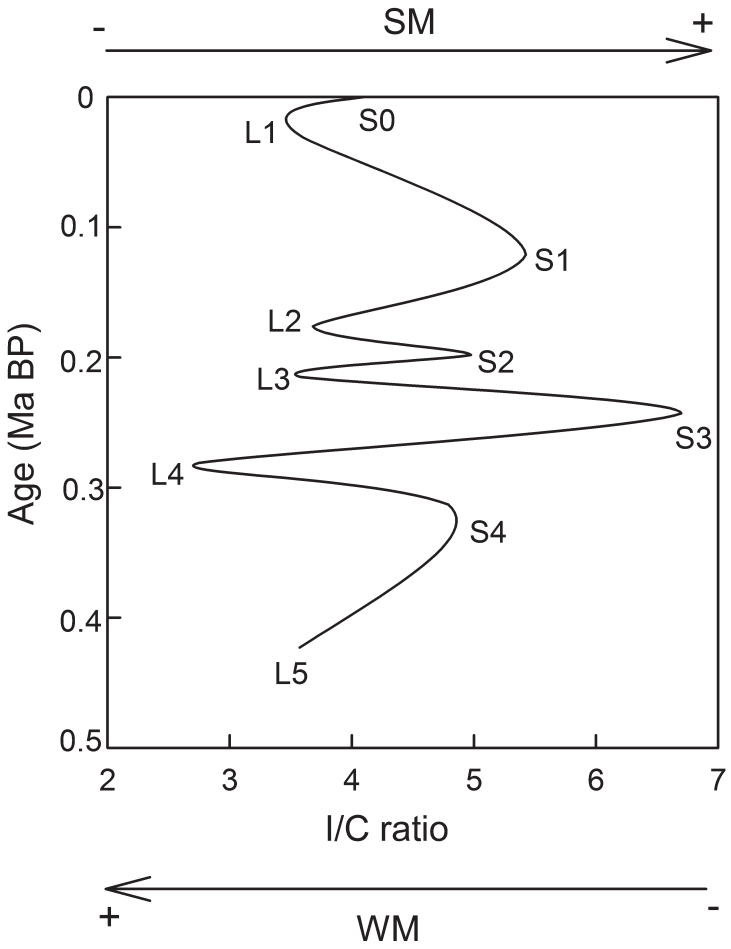

Figure 6 The trends in regional monsoon climate variability and change in the Chaoyang section, obtained from integrating data of clay using a time series with a moving average. The continuous line is the smoothed data using a moving average function. Here, the I/C (illite/chlorite) ratio model was employed as an integrated index to evaluate the monsoon influence (Chamley 1989; Zhao 2005). SM = summer monsoon influence; WM = winter monsoon strength.

weathering has had a marked effect on illite content (Gylesjö & Arnold 2006). The phyllosilicate composition does exhibit some differences between loess and palaeosols. The average illite content is higher in palaeosols as compared to loess. The most developed soil, as expressed in degree of weathering, has the greatest illite content; as in the Lingtai and Baoji sections, but also for the S3 palaeosol in the Chaoyang section. This, together with the relatively lower abundances of chlorite in palaeosols, may indicate that weathering mainly associates with illite through pedogenesis (Kalm *et al.* 1996). Thus, palaeosols with an average illite content of 61 % have experienced more intensive mineral weathering under a humid-warm climate than loess (38 %) during 0–0.423 Ma BP. At a large scale, there is an increased illite content from north to south, when the three loess sections at Chaoyang (48 %), Lingtai (49 %) (Gylesjö & Arnold 2006) and Baoji (66 %) (Kalm *et al.* 1996) are compared. The differences in illite from north to south indicate a trend of increased weathering.

Lower abundances of smectite were detected in the palaeosol when compared to the loess, and an abrupt decrease is exhibited from L2 to S1, as well as in the Lingtai and Wugong sections, during the last 0.423 Ma BP. This is likely due to the high permeability in most aeolian sediments that favours leaching of secondary minerals and chemical weathering (Chamley 1989). This difference may be triggered by an increase in base cation leaching (Borchardt 1989), due to the increased precipitation in S1. The difference coincides with the increase in vermiculite in S1, whose formation is favoured due to the interlayer K^+ cations that are removed from mica by increased leaching (Folkoff & Meentemeyer 1987). This means that loess formed under a dry climate has been subject to less leaching, whereas a palaeosol formed under a wet climate has had greater leaching (Beaven & Dumbleton 1966; Birkeland 1969; Ojanuga 1979).

S3 has a striking colour difference and has likely been subjected to relatively strong pedogenesis (Sun *et al.* 2016). Contrary to expectations, the kaolinite contents were the lowest in S3, which is one of the most developed layers in the Chaoyang section, and displays the same pattern in the Lingtai (Gylesjö & Arnold 2006) and Baoji sections (Kalm *et al.* 1996). An opposite trend can be observed in the clay content with depth (Fig. 4). The reason is that the constant addition of aeolian dust with high base saturation materials has restricted palaeosol weathering intensity over time (Sun *et al.* 2016). Weathering contributes greatly to differences in illite content. Further weathering of soil material was suppressed, due to the maintainance of high base saturation conditions for the constant addition of aeolian dust. Changes in source area mineralogy may play a more important role in the variability of kaolinite in S3 during 0.225–0.243 Ma BP than do changes in pedogenesis.

S0 shows the lowest illite concentration in the whole Chaoyang section and displays significantly less vermiculite. This may be due to an effect of water redistribution on the surface creating a dissimilar and altered parent material. Chen *et al.* (2009b) suggest that S0 has experienced some secondary reworking by local slope processes, including transportation by water during the Holocene. The dominant grain size fraction is 10–50 μm,

https://doi.org/10.1017/S1755691016000098 Published online by Cambridge University Press

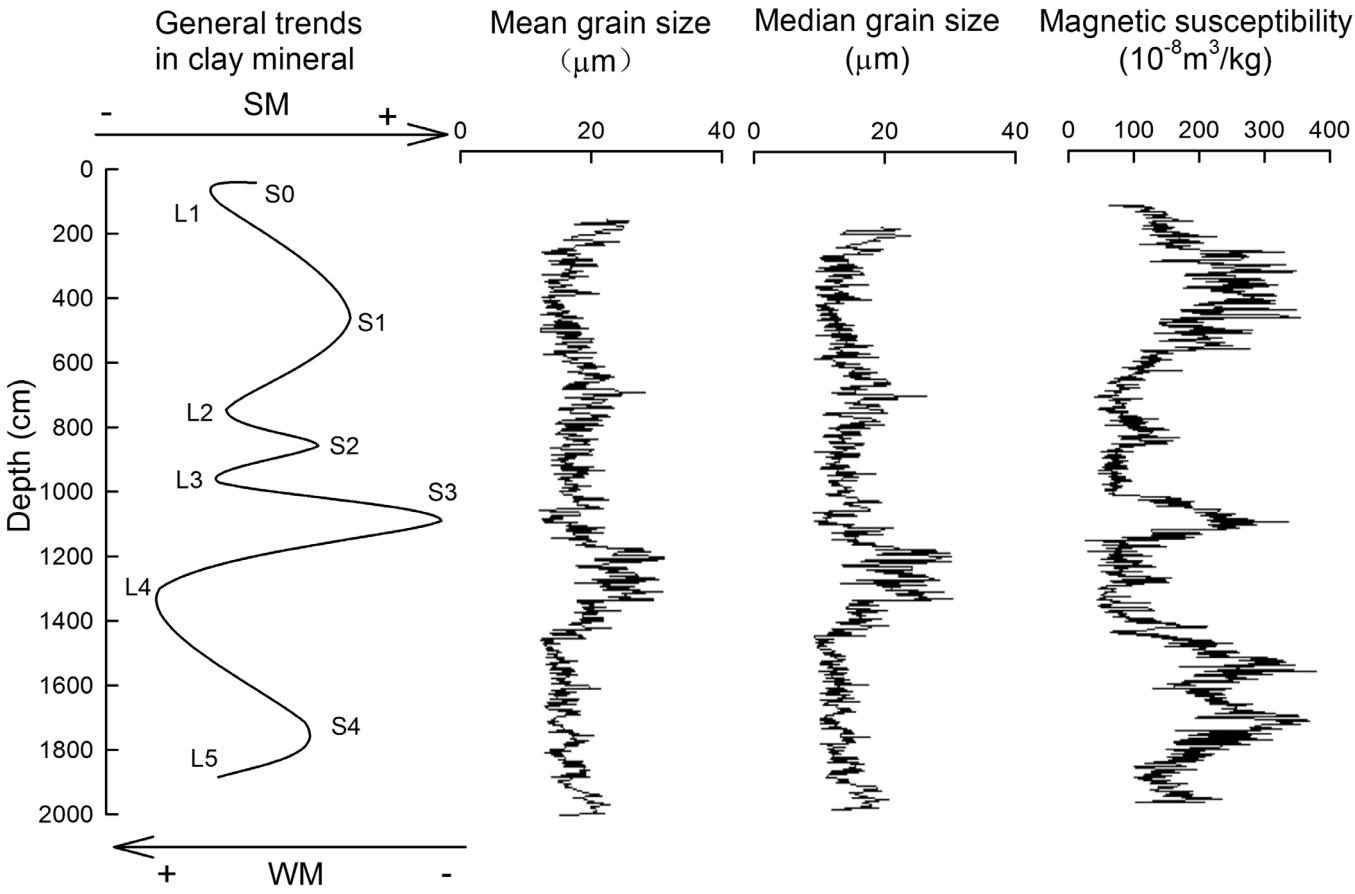

Figure 7 Variations in clay minerals compared to mean grain size, median grain size and magnetic susceptibility data in the Chaoyang loess–palaeosol sequence. The section above 2 m was reworked by water.

which is common in aeolian loess. However, a fluctuating and relatively large content of coarse size sands, together with a larger median size, indicates greater transport energy which exceeds the limits of aeolian wind speeds for loess deposits (Liu 1985; Sun *et al.* 2000). Hence, the absolute concentrations of illite probably changed substantially along with the introduction of the coarse size fraction. This would explain the relatively lower percentage of illite in the clay fractions of S0. Although the absolute content of illite was less in S0 than its actual value, the relative content in clay changed little, because the amount of total phyllosilicates was relatively low. Therefore, the trends and variations in illite within the different sections must be evaluated in the context of other data and our understanding of depositional processes.

L4 has the least illite content, and one of the greatest smectite concentrations and lowest chlorite abundance. The trend for more illite in cooler wetter climates may be used to infer that L4 has been subject to weak leaching and weathering, as well as cold-dry conditions; therefore, L4 may represent one of the coldest and driest periods during the last 0.423 Ma BP. We can infer that interlayer K^+ was extracted from the unit structure of mica as the soil was becoming very dry (Scott & Smith 1968), which created conditions for the greatest vermiculite content within the drier climate. As there is a weak relationship between chlorite content and climate (Folkoff & Meentemeyer 1987), the lowest concentration of chlorite present here is limited to the L4 that was weakly developed loess and commonly formed in cooler climates (Gao & Chen 1983; Yemane *et al.* 1996).

From L4 to S4, the illite content increases from 34 % (L4) to 66 % (S4). The trend in illite in S4 first decreases, then increases and, finally, decreases (Fig. 4). This suggests that the weathering environment, including temperature and precipitation conditions, changed during 0.311–0.243 Ma BP of S4 formation. This accords with Wang & Zheng (1989), in that a dry environment alternating with periods of moist conditions can be inferred from the illite content within the range 65–80 %.

In summary as shown in Figure 6, the palaeosols correlate with a strengthened summer monsoon, whereas the loess correlates with a strengthened winter monsoon. This suggests that the 0.225–0.243 Ma BP period was characterised by the strongest summer monsoon, whereas 0.243–0.311 Ma BP had the strongest winter monsoon. The climate was warm and wet at the following stages: 0.071–0.159 Ma BP, 0.176–0.208 Ma BP, 0.225–0.243 Ma BP and 0.311–0.403 Ma BP; and the climate was cold and dry at the following stages: 0.159–0.176 Ma BP, 0.208–0.225 Ma BP, 0.243–0.311 Ma BP and 0.403–0.423 Ma BP.

3.3. Magnetic susceptibility and grain size related to clay mineralogy

Magnetic susceptibility can serve as an important environmental proxy for pedogenic intensity in aeolian deposits and changes in the East Asian summer monsoon throughout the Quaternary (Zhou *et al.* 1990; An *et al.* 1991a; Maher & Thompson 1991). Greater magnetic susceptibility values can indicate a stronger summer monsoonal influence (Ding & Yu 1995). Research on the grain size features of the loess–palaeosol sequence has shown that greater amounts of the coarse fraction and a coarser median grain size are generally the result of a stronger Asian winter monsoon (Liu 1985; An *et al.* 1991a; Xiao *et al.* 1992; Ding *et al.* 1994; Zhang *et al.* 1994; An & Porter 1997; Lu & An 1998). Consequently, grain size parameters

https://doi.org/10.1017/S1755691016000098 Published online by Cambridge University Press

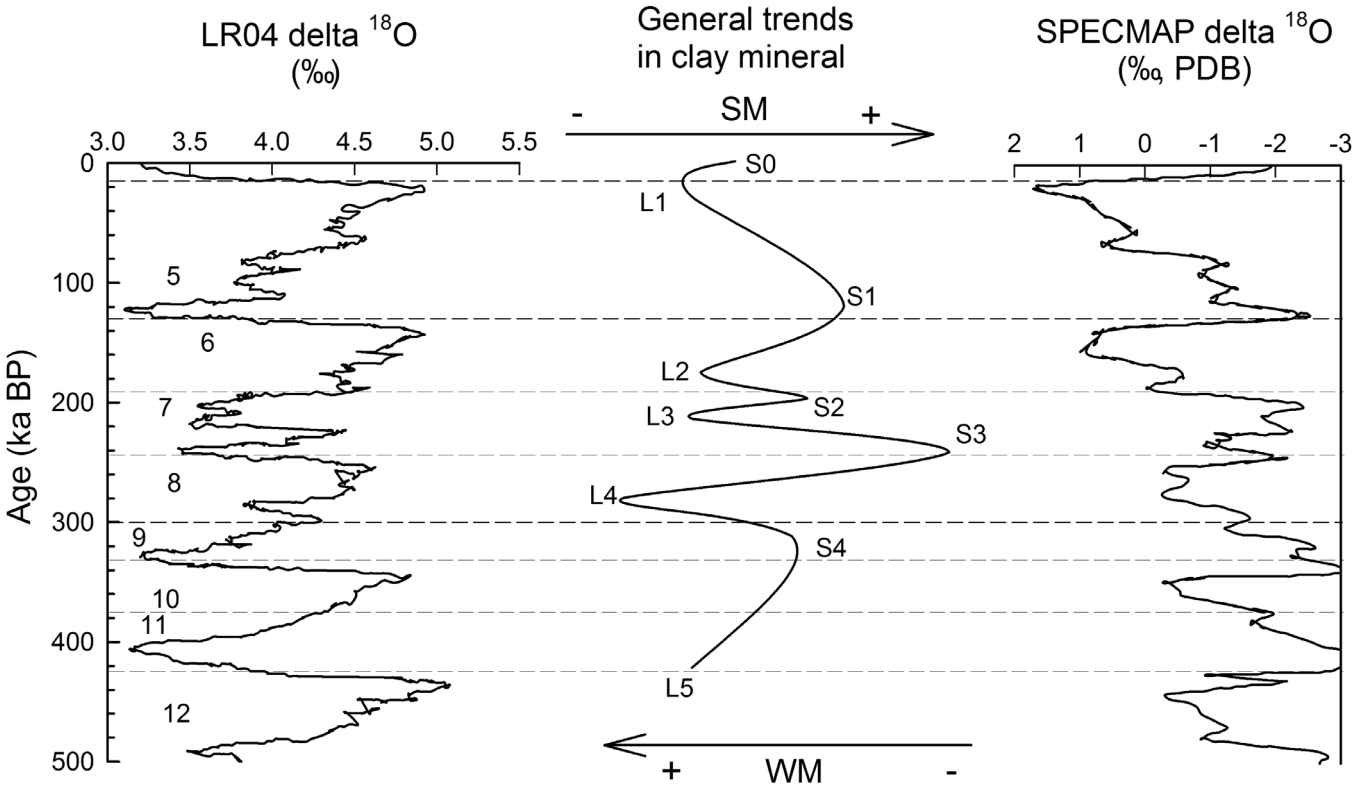

Figure 8 General clay mineral trends in the Chaoyang section and correlation with LR04 δ^{18}O (‰) records from Lisiecki & Raymo (2005) and SPECMAP δ^{18}O records (Martinson *et al.* 1987). The figures of LR04 δ^{18}O (‰) and SPECMAP δ^{18}O were obtained from a figure which was cited from Ding & Yu (1995).

(Ding *et al.* 2002), such as mean or median grain size, can be used as proxy indicators to reconstruct variations in the influence of the winter monsoon (Vandenberghe *et al.* 1997). Interpretations of a stronger influence of the winter monsoon can be based on coarser median grain size and mean grain size.

As shown in Figure 7, changes in clay minerals correlate well with the variations in magnetic susceptibility, median grain size and mean grain size suggestive of pedogenic cycles. Variations in clay minerals reflect a series of monsoonal changes, which are also reflected in both grain size distribution and magnetic susceptibility. Fluctuations in the intensity of the East Asian winter and summer monsoons are expressed in a shift in the same phase between grain size and magnetic susceptibility. Lesser values of magnetic susceptibility, and of the I/C ratio and a coarser median and mean grain size, were detected in loess. On the other hand, greater values of magnetic susceptibility and of the I/C ratio and a finer median and mean grain size were observed in palaeosols (Fig. 7). The fluctuations in the loess–palaeosol sequence at Chaoyang show the same trends as at Lingtai, which suggests strong winter monsoons alternating with strong summer monsoons.

3.4. Trends in the monsoon climate

From the base of L5 to the base of S4 there is (1) a decrease in illite; (2) an increase in smectite and chlorite; and (3) an increase in illite and a decrease of chlorite. The same trends can be observed in clay but are much less than in S4 (Fig. 4). The trend in clay in L5 indicates that the winter monsoon influence became stronger during the period characterised by decreases in illite, and then an increasing summer monsoon influence occurred towards the base of S4, during the period characterised by increased illite in L5. But the period of 0.423–0.403 Ma BP was still mainly controlled by the winter monsoon climate. The L5 formation period of 0.423–0.403 Ma BP correlates well to MIS12, with an increasing ice volume reflected both in the SPECMAP δ^{18}O curve (Imbrie *et al.* 1984) and the LR04 δ^{18}O curve (Lisiecki & Raymo 2005) (Fig. 8).

In the S4–L4 portion of the Chaoyang section, clay, illite and kaolinite concentrations decrease between S4 and the overlying L4 unit (Fig. 4). L4 is represented by the least illite concentration and one of the least kaolinite concentrations which, as one of the most stable phyllosilicates, is often used as an indicator of weathering (Bühmann 1994).

The strength of winter and summer monsoons shifts synchronously (Liu & Ding 1992; An & Porter 1997). This suggests that weaker weathering, triggered by climatic deterioration with a weak summer monsoon and a strong winter monsoon, occurred during 0.311 to 0.243 Ma BP. The occurrence of the greatest amount of coarse grains (19.9–52.6 μm) and least amount of super-fine grains (0.5–1.0 μm) (Chen *et al.* 2009a) can indicate the winter monsoon influence and summer monsoon strength, respectively (Liu & Ding 1998).

The general trends in clay content of L4 parallel those of MIS8, both in the SPECMAP δ^{18}O (Imbrie *et al.* 1984) and the LR04 δ^{18}O curves (Lisiecki & Raymo 2005) (Fig. 8), which indicates a larger oceanic ice volume and, also, significant cold weather at the global scale. From 0.423 to 0.243 Ma BP, the summer monsoon influence decreased and the winter monsoon grew stronger to peak at L4, coinciding with the increasing percentage of coarse grains.

The section from the top of L4 to the top of S3 (0.243–0.225 Ma BP) is characterised by an increase in illite to a maximum of around 77 % at S3 in the entire Chaoyang section; the same trend described in the Lingtai and Baoji sections during the last 0.423 Ma BP. Changes in the illite content within 65–80 % imply that periods of a dry environment alternated with periods of moist conditions (Wang & Zheng 1989). In S3 of the Chaoyang section, there is only one clearly defined soil. This is because of the small accumulation rate and, thus, Chaoyang appears to reflect a shorter period under a sub

https://doi.org/10.1017/S1755691016000098 Published online by Cambridge University Press

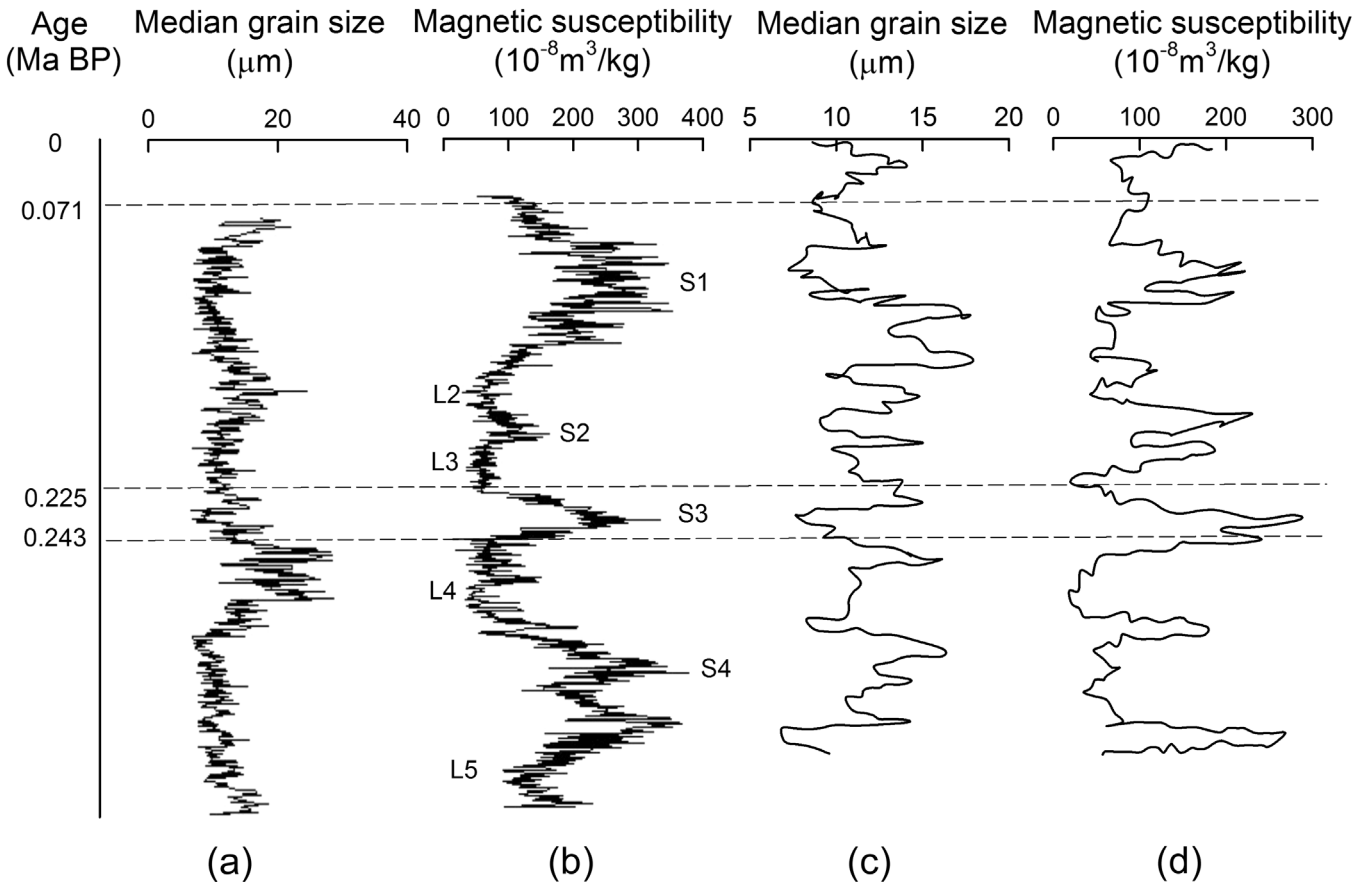

Figure 9 Median grain size and magnetic susceptibility in the Chaoyang section (a, b) corresponded to general trends in the Lingtai section (c, d). (c) and (d) were obtained from a figure cited from Gylesjö & Arnold (2006).

wet-dry-climate during 0.243–0.225 Ma BP. The summer monsoon influence grew more marked as the illite content increases to the maximum at S3, followed by a substantial increase in the clay coincident with an increase in fine grain sizes (Chen *et al.* 2009a). This correlates with the oxygen isotopic data from deep-sea records of MIS7, both in the SPECMAP $\delta^{18}O$ curve and in the LR04 curve (Fig. 8).

From the top of S3 to the base of S1, another decrease in illite is accompanied by a significant decrease in the concentrations of vermiculite and an increase in chlorite, together with a decrease in concentrations of clay (Fig. 4). This illustrates that there is also a decrease in the summer monsoon strength and an increase in the winter monsoon influence. This is consistent with the decrease in the abundance of coarse grains (as an indicator of the winter monsoon) and the increase in super-fine grains (as an indicator of the summer monsoon), which matches well with MIS7 and MIS6 (Fig. 8).

The relatively thick S1 has an increased illite, kaolinite and smectite contents, with a smaller chlorite concentration. This provides evidence for a major shift from a cold to a mild continental climate from L2 to S1, which coincides with the changes in concentrations of coarse and super-fine grains. These observations suggest a stronger summer monsoon. Palaeosol S1 interbedded between L1 and L2 is consistent with a period of relatively mild climate during 0.159–0.071 Ma BP. However, there is a relative increase in smectite in L1 and L2, which illustrates that the presence of greater amounts of K, Na and an increased pH could be needed to promote smectite genesis (Wilson 1987; Pickering 1986). The mean annual temperature and the mean annual precipitation were reported as greater than 9.1°C and 600 mm respectively, should a summer monsoon have occurred between 0.159 and 0.071 Ma BP (S1), with a temperature and precipitation that exceeded that of the modern climates of the Lingtai section (N 35°00′75″, E 107°30′33″; 9.1°C, 600 mm) and of the Baoji section (N 34°24′, E 107°18′; 13°C, 700 mm).

A major change occurs in the Chaoyang section in terms of mineralogy across S1–L5 to the L1 boundary around 0.071 Ma BP. From the boundary of S1 to L1, there is a significant decrease in illite and clay, whilst an increase in chlorite also can be observed. This illustrates a stronger winter than summer monsoonal influence, which is consistent with grain size characteristics, and may correspond to MIS5/4. Rousseau & Kukla (2000) and Gylesjö & Arnold (2006) also conclude that there was a weaker summer monsoon at the boundary across S1 to L1 at 0.071 Ma BP.

Palaeosols S4–S1 have greater average illite and kaolinite amounts than L2–L5 loess. This may reflect increased weathering contributing to the illite abundance under a stronger summer monsoon influence within S4–S1. The same trends were observed by Ding *et al.* (1999) and Gylesjö & Arnold (2006). Since chlorite is unstable in soils, the increased chlorite content can imply a decrease in weathering intensity (Righi *et al.* 1995). But sometimes the average chlorite abundances and smectite contents do not correlate well with the trends in illite, magnetic susceptibility and grain size. Variations in source mineralogy are sometimes more important than pedogenesis in explaining chlorite content, as also proposed by Gylesjö & Arnold (2006) for the Lingtai section. An increase in chlorite, as well as an increase in coarse grains, suggests that the wind speed during the winter monsoon had a greater intensity. The average chlorite abundance within S1–L5 in the Chaoyang section is greater than at Lingtai and Baoji, suggesting a drier environment at Chaoyang.

https://doi.org/10.1017/S1755691016000098 Published online by Cambridge University Press

3.5. Determining the specific position for S3 over the last 2.6 Ma BP

Since clay mineral data should not be used on their own, magnetic susceptibility and median grain size data are also considered, in order to propose the position of the summer monsoon during 0.225–0.243 Ma BP. In Figure 9, magnetic susceptibility and median grain size in the Chaoyang section agree very well with the Lingtai section. As discussed above, S3 was characterised by clay mineral features as the strongest summer monsoon in the last 0.423 Ma BP, and indicates some possibilities for its position during the last 2.6 Ma BP. In general, the largest amplitude in variation can be observed around S3 at Chaoyang, as well as at Lingtai, and seems to correlate well with the lowest peak in the time series of median grain size, the highest magnetic susceptibility (Fig. 9), illite abundances (Fig. 4) and the I/C ratio (Fig. 7).

This also can imply that the strongest summer monsoon occurred in S3 in the last 0.423 Ma BP, coinciding with Lingtai. Ding *et al.* (1999) determined that the strongest summer monsoon occurred in the last 0.48 Ma BP, on the basis of the pedogenic characteristics in the last 2.6 Ma BP. Through comparison with the median grain size and magnetic susceptibility data from Lingtai (Fig. 9), we can propose that one of the strongest summer monsoons during the last 2.6 Ma BP was during 0.225–0.243 Ma BP.

Some mineral differences may be due to local factors such as temperature and moisture in the same period. Even in modern soil, these differences can be observed. The general trends in the mineralogical changes closely correlate with the climatic trends, as determined using CLP loess–palaeosol sequences and ice volume features in oxygen isotopes from deep-sea records. This implies that the Chaoyang section provides a detailed record of palaeoclimate change in northeast China.

4. Conclusions

1. The clay mineralogy in the Chaoyang section records the development of the loess–palaeosol sequence. In the Chaoyang section, illite (40–70 %) dominates the clay fraction, as compared to vermiculite (20–40 %), kaolinite (6–15 %) and chlorite (2–15 %), with minor amounts of smectite (0–10 %) throughout the entire section. A greater variability can be generally observed within palaeosols as compared to loess, with the largest and smallest amounts of different minerals in S3 and L4 respectively. The increase in pedogenic processes, or the lack of pedogenic processes, strongly controlled illite evolution. In general, the palaeosols contain more illite, total clay and kaolinite, together with less chlorite than in the loess. The variations in phyllosilicate composition of loess–palaeosol sequences indicate temporal and spatial changes in mineral evolution and the strength of the summer/winter monsoon. Of course, there were potential influences from the local environment; but, nevertheless, we observed differences in mineral variation for the period 0–0.071 Ma BP, despite different thicknesses of the lithologic units among the Chaoyang, Lingtai and Baoji sections. However, the general trends of mineralogical changes are synchronous with the distinctive mineralogical trends in the CLP.
2. Based on the mineralogical composition and the clay content of each horizon in the Chaoyang section, the paleoclimate changes over the last 0.423 Ma BP in the Chaoyang area can be summarised. From 0.423 Ma BP to 0.243 Ma BP, the summer monsoon influence decreased and the winter monsoon grew stronger. The strongest winter monsoon was found to occur during 0.311–0.243 Ma BP. Between 0.243 Ma BP and 0.225 Ma BP, the strength of the summer monsoon started to increase again, which was one of the strongest summer monsoons in the last 2.6 Ma BP. From 0.225 Ma BP to 0.071 Ma BP, a decrease in the summer monsoon strength and an increase in the winter monsoon influence occurred. At 0.071 Ma BP, the summer monsoon strength decreased.
3. The reconstruction of the palaeoclimate, based on the Chaoyang section and using the clay mineral proxy, accords with proxies including magnetic susceptibility, median grain size and mean grain size, and has a very high similarity to the glacial–interglacial cycles, as reflected in the marine $\delta^{18}O$ records as well as in the loess-palaeosol sections in the CLP. These relationships further suggest that the Chaoyang section provides a record for global climate changes. Palaeoclimate variations as recorded in the Chaoyang section complement records from the CLP and contribute significantly to a better understanding of global paleoclimate changes during the Late Middle Pleistocene.

5. Acknowledgments

The authors sincerely thank Professor Donald Davidson, University of Stirling, UK, for reviewing an earlier version of the paper; Martha R. Winters at Purdue University, USA, for language help; and all the students and staff who provided their input to this study. Thanks also go to the National Natural Science Foundation of China (No. 40971124 and No. 41371223) and the China Scholarship Council (201408210121 and 201508210201) for funding this project. Our acknowledgements also extended to the two anonymous reviewers for their constructive reviews of the manuscript.

6. References

Ackerley, D., Booth, B. B. B., Knight, S. H. E., Highwood, E. J., Frame, D. J., Allen, M. R. & Rowell, D. P. 2011. Sensitivity of twentieth-century Sahel rainfall to Sulfate aerosol and CO_2 forcing. *Journal of Climate* **24**(19), 4999–5014.

Amundson, R. G., Doner, H. E., Chadwick, O. A. & Sowers, J. M. 1989. The stable isotope chemistry of pedogenic carbonates at Kyle Canyon, Nevada. *Soil Science Society of America Journal* **53**(1), 201–10.

An, Z. S. 2000. The history and variability of the East Asian paleomonsoon climate. *Quaternary Science Reviews* **19**(1), 171–87.

An, Z. S., Kukla, G., Porter, S. C. & Xiao, J. L. 1991a. Late Quaternary dust flow on the Chinese loess plateau. *Catena* **18**(2), 125–32.

An, Z. S., Kukla, G. J., Porter, S. C. & Xiao, J. L. 1991b. Magnetic susceptibility evidence of monsoon variation on the Loess Plateau of central China during the last 130,000 years. *Quaternary Research* **36**(1), 29–36.

An, Z. S. & Porter, S. C. 1997. Millennial-scale climatic oscillations during the last interglaciation in central China. *Geology* **25**(7), 603–06.

Arkley, R. J. 1963. Calculation of carbonate and water movement in soil from climatic data. *Soil Science* **96**(4), 239–48.

Arkley, R. J. 1967. Climates of some great soil groups of the western United States. *Soil Science* **103**(6), 389–400.

Bühmann, C. 1994. Parent material and pedogenic processes in South Africa. *Clay Minerals* **29**(2), 239–46.

Beaven, P. J. & Dumbleton, M. J. 1966. Clay minerals and geomorphology in four Caribbean islands. *Clay Minerals* **6**, 371–82.

Bekryaev, R. V., Polyakov, I. V. & Alexeev, V. A. 2010. Role of polar amplification in long-term surface air temperature variations and modern arctic warming. *Journal of Climate* **23**(14), 3888–906.

Birkeland, P. W. 1969. Quaternary paleoclimatic implications of soil clay mineral distribution in a Sierra Nevada-Great Basin transect. *The Journal of Geology* **77**, 289–302.

Borchardt, G. 1989. Smectites. *In* Dixon, J. B. & Weed, S. B. (eds) *Minerals in Soil Environment*. *SSSA Book Series* **1**, 675–727. Madison, Wisconsin: Soil Science Society of America Inc. 1244 pp.

Brindley, G. W. 1980. Quantitative X-ray mineral analysis of clays. *In* Brindley, G. W. & Brown, G. (eds) *Crystal Structures of Clay*

Minerals and their X-Ray Identification. Mineralogical Society Monograph **5**, 411–38. London: Mineralogical Society of Grear Britain and Ireland.

Brown, G. & Brindley, G. W. 1980. X-ray diffraction procedures for clay mineral identification. *In* Brindley, G. W. & Brown, G. (eds) *Crystal structures of clay minerals and their X-ray identification*, 305–59. London: Mineralogical Society.

Chadwick, O. A., Nettleton, W. D. & Staidl, G. J. 1995. Soil polygenesis as a function of Quaternary climate change, northern Great Basin, USA. *Geoderma* **68**(1), 1–26.

Chadwick, O. A., Gavenda, R. T., Kelly, E. F., Ziegler, K., Olson, C. G., Elliott, W. C. & Hendricks, D. M. 2003. The impact of climate on the biogeochemical functioning of volcanic soils. *Chemical Geology* **202**(3–4), 195–223.

Chamley, H. 1989. *Clay Sedimentology*: Springer-Verlag. 623 pp.

Chen, H. 2009. [*Grain-Size Characteristics and Paleoclimatic Reconstruction during the Late Middle Pleistocene and the last interglacial stage of a Palaeosol Sequence at Fenghuang Mountain in Chaoyang, Liaoning Province.*] [In Chinese.] PhD Thesis, Shenyang Agricultural University.

Chen, H., Wang, Q. B. & Han, C. L. 2009a. Grain-size characteristics and climatic changes of a palaeosol sequence at Fenghuang Mountain in Chaoyang, Liaoning Province *Geological Journal of China Universities* **15**, 563–68.

Chen, H., Wang, Q. B., Han, C. L. & Wu, D. L. 2009b. Grain-size distribution and material origin of a palaeosol sequence at Fenghuang Mountain, Chaoyang, Liaoning Province *Earth and Environment* **37**(3), 243–48.

Ding, Z. L., Yu, Z. W., Rutter, N. W. & Liu, T. S. 1994. Towards an orbital time scale for Chinese loess deposits. *Quaternary Science Reviews* **13**(1), 39–70.

Ding, Z. L., Xiong, S. F., Sun, J. M., Yang, S. L., Gu, Z. Y. & Liu, T. S. 1999. Pedostratigraphy and paleomagnetism of a ~7.0 Ma eolian loess-red clay sequence at Lingtai, Loess Plateau, north-central China and the implications for paleomonsoon evolution. *Palaeogeography, Palaeoclimatology, Palaeoecology* **152**(1), 49–66.

Ding, Z. L., Sun, J. M., Yang, S. L. & Liu, T. S. 2001. Geochemistry of the Pliocene red clay formation in the Chinese Loess Plateau and implications for its origin, source provenance and paleoclimate change. *Geochimica et Cosmochimica Acta* **65**(6), 901–13.

Ding, Z. L., Derbyshire, E., Yang, S. L., Yu, Z. W., Xiong, S. F. & Liu, T. S. 2002. Stacked 2.6-Ma grain size record from the Chinese loess based on five sections and correlation with the deep-sea δ^{18}O record. *Paleoceanography* 17(3), 5-1–5-21.

Ding, Z. L. & Yu, Z. W. 1995. Forcing mechanisms of paleomonsoons over East Asia. *Quaternary Sciences* **1**, 63–74.

Dixon, J. B. & Weed, S. B. 1989. *Minerals in Soil Environments*. Madison, Wisconsin: Soil Science Society of America Inc. 1244 pp.

Dole, R. M. 2012. *Toward understanding and predicting regional climate variations and change*. (Findings from NOAA Science Challenge Workshop 2011). Boulder, Colorado: NOAA. 32 pp.

Feng, J. L., Hu, Z. G., Ju, J. T. & Zhu, L. P. 2011. Variations in trace element (including rare earth element) concentrations with grain sizes in loess and their implications for tracing the provenance of eolian deposits. *Quaternary International* **236**(1–2), 116–26.

Fink, J. & Kukla, G. J. 1977. Pleistocene climates in Central Europe: at least 17 interglacials after the Olduvai event. *Quaternary Research* **7**(3), 363–71.

Fiskell, J. G. & Perkins, H. 1970. Selected coastal plain soil properties. *Southern Cooperative Bulletin* **148**. Gainesville: University of Florida.141 pp.

Folkoff, M. E. & Meentemeyer, V. 1985. Climatic control of the assemblages of secondary clay minerals in the A-horizon of United States soils. *Earth Surface Processes and Landforms* **10**(6), 621–33.

Folkoff, M. E. & Meentemeyer, V. 1987. Climatic control of the geography of clay minerals genesis. *Annals of the Association of American Geographers* **77**(4), 635–50.

Gao, Y. X. & Chen, H. Z. 1983. Salient characteristics of soil-forming processes in Xizang (Tibet). *Soil Science* **135**(1), 11–17.

Gibbs, R. J. 1965. Error due to segregation in quantitative clay mineral X-ray difraction mounting techniques. *American Mineralogist* **50**, 741–51.

Grim, R. E. 1968. *Clay mineralogy*, 2nd Edition. New York: McGraw-Hill. 596 pp.

Gylesjö, S. & Arnold, E. 2006. Clay mineralogy of a red clay–loess sequence from Lingtai, the Chinese Loess Plateau. *Global and Planetary Change* **51**(3–4), 181–94.

Hall, R. D. & Anderson, A. K. 2000. Comparative soil development of Quaternary palaeosols of the central United States. *Palaeogeography, Palaeoclimatology, Palaeoecology* **158**(1), 109–45.

Heller, F. & Liu, T. S. 1982. Magnetostratigraphical dating of loess deposits in China. *Nature* **300**, 431–33.

Hu, X.-F., Wei, J., Du, Y., Xu, L.-F., Wang, H.-B., Zhang, G.-L., Ye, W. & Zhu, L.-D. 2010. Regional distribution of the Quaternary Red Clay with aeolian dust characteristics in subtropical China and its paleoclimatic implications. *Geoderma* **159**(3–4), 317–34.

Huang, C. Q., Zhao, W., Liu, F., Tan, W. F. & Koopal, L. K. 2011. Environmental significance of mineral weathering and pedogenesis of loess on the southernmost Loess Plateau, China. *Geoderma* **163**(3–4), 219–26.

Huang, C. Q., Zhao, W., Li, F. Y., Tan, W. F. & Wang, M. K. 2012. Mineralogical and pedogenetic evidence for palaeoenvironmental variations during the Holocene on the Loess Plateau, China. *Catena* **96**, 49–56.

Imbrie, J., Hays, J. D., Martinson, D. G., Mcintyre, A., Mix, A. C., Morley, J. J., Pisias, N. G., Prell, W. L. & Shackleton, N. J. 1984. The orbital theory of Pleistocene climate: Support from a revised chronology of the marine δ^{18}O record. *In* Berger, A. L., Imbrie, J., Hays, J. , Kukla, G. & Saltzman, B. (eds) *Milankovitch and Climate: Understanding the Response to Astronomical Forcing,* 269. (Proceedings of the NATO Advanced Research Workshop, Palisades, New York, U.S.A., November 30–December 4, 1982.) Springer. 946 pp.

Jansen, E., Overpeck, J., Briffa, K. R., Duplessy, J. C., Joos, F., Masson-Delmotte, V., Olago, D., Otto-Bliesner, B., Peltier, W. R., Rahmstorf, S., Ramesh, R., Raynaud, D., Rind, D., Solomina, O., Villalba, R. & Zhang, D. 2007. Palaeoclimate. *In* Solomon, S., Qin, D., Manning, M., Chen, Z., Marquis, M., Averyt, K. B., Tignor, M. & Miller, H. L. (eds) *Contribution of Working Group I to the Fourth Assessment Report of the Intergovernmental Panel on Climate Change . limate Change 2007: The Physical Science Basis.* Cambridge, UK and New York, USA: Cambridge University Press.

Jeong, G. Y., Hillier, S. & Kemp, R. A. 2008. Quantitative bulk and single-particle mineralogy of a thick Chinese loess–palaeosol section: implications for loess provenance and weathering. *Quaternary Science Reviews* **27**(11–12), 1271–87.

Jeong, G. Y., Hillier, S. & Kemp, R. A. 2011. Changes in mineralogy of loess–palaeosol sections across the Chinese Loess Plateau. *Quaternary Research* **75**(1), 245–55.

Kalm, V. E., Rutter, N. W. & Rokosh, C. D. 1996. Clay minerals and their paleoenvironmental interpretation in the Baoji loess section, Southern Loess Plateau, China. *Catena* **27**(1), 49–61.

Kukla, G. 1987. Loess stratigraphy in central China. *Quaternary Science Reviews* **6**(3), 191–219.

Kukla, G. & An, Z. S. 1989. Loess stratigraphy in central China. *Palaeogeography, Palaeoclimatology, Palaeoecology* **72**, 203–25.

Li, G. J., Ji, J. F., Zhao, L., Mao, C. P. & Chen, J. 2008. Response of silicate weathering to monsoon changes on the Chinese Loess Plateau. *Catena* **72**(3), 405–12.

Li, X. Y. 1997. *Soil chemistry and experiment guidance*. Beijing: China Agriculture Press.

Liaoning Geology Bureau, Hydrogeology Brigade. 1983. *The Quaternary of Liaoning Province*, 46–62. Beijing: Geology Press.

Lisiecki, L. E. & Raymo, M. E. 2005. A Pliocene–Pleistocene stack of 57 globally distributed benthic δ^{18}O records. *Paleoceanography* **20**(1), 1–17.

Liu, T. S. 1985. *Loess and the Environment*, 31–148. Beijing: China Ocean Press. 251 pp.

Liu, T. S. & Ding, Z. L. 1992. The stage coupling process of monsoon circulation and continental ice volume changes over the last 2.5 Ma. *Quaternary Sciences* **1**, 12–23.

Liu, T. S. & Ding, Z. L. 1998. Chinese loess and the paleomonsoon. *Annual Review of Earth and Planetary Sciences* **26**(1), 111–45.

Lu, H. Y. & An, Z. S. 1998. Paleoclimatic significance of grain size of loess-palaeosol sequences of central China *Science China, Series D: Earth Science* **41**, 626–31.

Maher, B. A. & Thompson, R. 1991. Mineral magnetic record of the Chinese loess and palaeosols. *Geology* **19**(1), 3–6.

Martinson, D. G., Pisias, N. G., Hays, J. D., Imbrie, J., Moore, T. C. & Shackleton, N. J. 1987. Age dating and the orbital theory of the ice ages: development of a high-resolution 0 to 300,000-year chronostratigraphy. *Quaternary Research* **27**(1), 1–29.

Mehra, O. P. & Jackson, M. L. 1958. Iron oxide removal from soils and clays by a dithionite-citrate system buffered with sodium bicarbonate. *In Clays and Clay Minerals. Proceedings of 7th Conference on Clays and Clay Minerals*, 317–327. Elsevier Ltd. 370 pp.

Mintzer, I. M. 1992. *Confronting Climate Change: Risks, Implications and Responses*. Cambridge University Press. 400 pp.

Moore, D. M. & Reynolds, R. C. 1989. *X-ray Diffraction and the Identification and Analysis of Clay Minerals*. Oxford: Oxford University Press. 332 pp.
Ojanuga, A. G. 1979. Clay mineralogy of soils in the Nigerian tropical savanna regions. *Soil Science Society of America Journal* **43**(6), 1237–42.
Pai, C. W., Wang, M. K., Wang, W. M. & Houng, K. H. 1999. Smectites in iron-rich calcareous soil and black soils of Taiwan. *Clays and Clay Minerals* **47**(4), 389–98.
Peng, H. 1988. A discussion on the formation of the red boulder clay in the Ranggiaoling of Loushan Mountain. *Journal of Geographical Sciences* **43**, 363–66.
Pickering, W. F. 1986. Metal ion speciation—soils and sediments (a review). *Ore Geology Reviews* **1**(1), 83–146.
Pye, K. 1984. Loess. *Progress in Physical Geography* **8**(2), 176–217.
Pye, K. 1987. *Aeolian dust and dust deposits*. London: Academic Press. 256 pp.
Rai, D. & Lindsay, W. L. 1975. A thermodynamic model for predicting the formation, stability, and weathering of common soil minerals. *Soil Science Society of America Journal* **39**(5), 991–96.
Righi, D., Velde, B. & Meunier, A. 1995. Clay stability in clay-dominated soil systems. *Clay Minerals* **30**(1), 45–54.
Rousseau, D. D. & Kukla, G. 2000. Abrupt retreat of summer monsoon at the S1/L1 boundary in China. *Global and Planetary Change* **26**(1), 189–98.
Schaetzl, R. J. & Anderson, S. 2005. *Soils: Genesis and geomorphology* New York: Cambridge University Press.
Scott, A. D. & Smith, S. J. 1968. Mechanism for soil potassium release by drying. *Soil Science Society of America Journal* **32**(3), 443–44.
Srodon, J. & Eberl, D. D. 1984. Illite. *Reviews in Mineralogy and Geochemistry* **13**(1), 495–544.
Sun, D. H., Lu, H. Y., Rea, D. & Sun, Y. B. 2000. Bi-mode grain-size distribution of Chinese Loess and its paleoclimate implication. *Acta Sedimentologica Sinica* **18**, 327–35.
Sun, Y. B., Lu, H. Y. & An, Z. S. 2006. Grain size of loess, palaeosol and Red Clay deposits on the Chinese Loess Plateau: Significance for understanding pedogenic alteration and palaeomonsoon evolution. *Palaeogeography, Palaeoclimatology, Palaeoecology* **241**(1), 129–38.
Sun, Z.-X., Owens, P. R., Han, C.-L., Chen, H., Wang, X.-L. & Wang, Q.-B. 2016. A quantitative reconstruction of a loess–palaeosol sequence focused on palaeosol genesis: An example from a section at Chaoyang, China. *Geoderma* **266**, 25–39.
Theisen, A. A. & Harward, M. E. 1962. A paste method for preparation of slides for clay mineral identification by X-ray diffraction. *Soil Science Society of America Journal* **26**(1), 90–91.
Thorez, J. 1976. *Practical identification of clay minerals: a handbook for teachers and students in clay mineralogy*. Dison: Lelotte. 90 pp.
Turpault, M. P., Righi, D. & Utérano, C. 2008. Clay minerals: Precise markers of the spatial and temporal variability of the biogeochemical soil environment. *Geoderma* **147**(3–4), 108–15.
Van Der Merwe, C. R. & Weber, H. W. 1963. The clay minerals of South African soils developed from granite under different climatic conditions. *South African Journal of Science* **6**, 411–54.
Vandenberghe, J., An, Z. S., Nugteren, G., Lu, H. Y. & Van Huissteden, K. 1997. New absolute time scale for the Quaternary climate in the Chinese loess region by grain-size analysis. *Geology* **25**(1), 35–38.
Velde, B. 2012. *Introduction to clay minerals: chemistry, origins, uses and environmental significance*, New York: Springer Science & Business Media.
Velde, B. & Meunier, A. 2008. *The origin of clay minerals in soils and weathered rocks*, Berlin, Heidelberg: Springer-Verlag.
Wang, S. 1988. Clay minerals and paleoclimate evolution in the Yangyuan Basin, Hebei Province. *Marine Geology Quaternary Geology* **8**, 77–90.
Wang, Y. & Zheng, S. H. 1989. Palaeosol nodules as Pleistocene paleoclimatic indicators, Luochuan, P. R. China. *Palaeogeography, Palaeoclimatology, Palaeoecology* **76**(1), 39–44.
White, A. F. & Blum, A. E. 1995. Effects of climate on chemical weathering in watersheds. *Geochimica et Cosmochimica Acta* **59**(9), 1729–47.
Wild, M. 2012. Enlightening global dimming and brightening. *Bulletin of the American Meteorological Society* **93**(1), 27–37.
Williams, A. P. & Funk, C. 2011. A westward extension of the warm pool leads to a westward extension of the Walker circulation, drying eastern Africa. *Climate Dynamics* **37**(11–12), 2417–35.
Wilson, M. J. 1987. Soil smectites and related interstratified minerals: Recent developments. *In* Schultz, L. G., Van Holphen, H. & Mumpton, F. A. (eds) *Proceedings of the International Clay Conference Denver 1985,* 167–73. Bloomington, ID: Clay Minerals Society.
Wilson, M. J. 1999. The origin and formation of clay minerals in soils: past, present and future perspectives. *Clay Minerals* **34**(1), 7–25.
Xiao, J. L., Zheng, H. B. & Zhao, H. 1992. Variation of winter monsoon intensity on the Loess Plateau, central China during the Last 130,000 years: Evidence from grain size distribution. *Quaternary Sciences* **31**(1), 13–19.
Yang, H. R. & Xu, Q. 1985. *The evolution of Quaternary natural environment in eastern China*, 104–25. Beijing: Geology Press.
Yemane, K., Kahr, G. & Kelts, K. 1996. Imprints of post-glacial climates and palaeogeography in the detrital clay mineral assemblages of an Upper Permian fluviolacustrine Gondwana deposit from northern Malawi. *Palaeogeography, Palaeoclimatology, Palaeoecology* **125**(1), 27–49.
Zhang, J. C. & Lin, Z. G. 1987. *Climate in China*. Beijing: Meteorology Press. 325 pp.
Zhang, N. X. & Yuan, B. Y. 1987. Study of clay minerals in Louchuan section and their paleoenvironment significance. *In* Liu Tungsheng (ed.) *Aspects of Loess Research,* 348–61. Beijing: China Ocean Press.
Zhang, X. Y., An, Z. S., Chen, T., Zhang, G. Y., Arimoto, R. & Ray, B. J. 1994. Late Quaternary records of the atmospheric input of eolian dust to the center of the Chinese Loess Plateau. *Quaternary Research* **41**(1), 35–43.
Zhao, L. 2005. Variations of illite/chlorite ratio in Chinese loess sections during the last glacial and interglacial cycle: Implications for monsoon reconstruction. *Geophysical Research Letters* **32**(20), 1–4.
Zheng, H. 1982. Paleoclimate events recorded in clay minerals in loess of China. *In* Liu Tungsheng (ed.) *Quaternary Geology and Environment of China,* 59–66. Beijing: China Ocean Press.
Zhou, L. P., Oldfield, F., Wintle, A. G., Robinson, S. G. & Wang, J. T. 1990. Partly pedogenic origin of magnetic variations in Chinese loess. *Nature* **346**, 737–39.

MS received 3 August 2015. Accepted for publication 4 June 2016